



Pergamon

Acta mater. 48 (2000) 4493–4499



www.elsevier.com/locate/actamat

THE IMPORTANCE OF AMORPHOUS INTERGRANULAR FILMS IN SELF-REINFORCED Si_3N_4 CERAMICS

P. F. BECHER*, G. S. PAINTER, E. Y. SUN‡, C. H. HSUEH and M. J. LANCE

Metals and Ceramics Division, Oak Ridge National Laboratory, Oak Ridge, TN 37831, USA

Abstract—High-fracture-strength and high-toughness $\beta\text{-Si}_3\text{N}_4$ ceramics can be obtained by tailoring the size and number of the elongated bridging grains. However, these bridging mechanisms rely on debonding of the reinforcing grains from the matrix to increase toughness. Interfacial debonding is shown to be influenced by sintering aids incorporated in the amorphous intergranular films. In one case, the interface strength between the intergranular glass and the reinforcing grains increases with the aluminum and oxygen content of an interfacial epitaxial $\beta\text{-SiAlON}$ layer. In another, the incorporation of fluorine in the intergranular film allows the crack to circumvent the grains. Atomic cluster calculations reveal that these two debonding processes are related to (1) strong Si–O and Al–O bonding across the glass/crystalline interface with an epitaxial SiAlON layer and (2) a weakening of the amorphous network of the intergranular film when difluorine substitutes for bridging oxygen. © 2000 Acta Metallurgica Inc. Published by Elsevier Science Ltd. All rights reserved.

Keywords: Ceramics; Interfaces; Microstructure; Toughness; Cluster calculations

1. BACKGROUND

There have been a number of observations of increases in the mechanical performance of silicon nitride ceramics associated with the formation of elongated grains; for example, the early studies by Himsolt *et al.* [1] and Lange [2]. Kawashima and co-workers [3] and Mitomo [4] provided evidence to show that the fracture toughness increased with the diameter of these elongated grains. More recent studies by Hirao and co-workers [5, 6] and Emoto and Mitomo [7] have shown that beta seeds can be used to control the size and volume fraction of elongated grains in these so-called self-reinforced ceramics. The toughening effect arises from deflection of the crack tip by these elongated grains and by subsequent generation of bridging grains in the wake of the crack tip, similar to what occurs in both whisker-reinforced [8–11] and fiber-reinforced [12] ceramics. The crack-bridging reinforcements dissipate considerable strain energy through friction generated by their motion against the matrix during elastic stretching along the debonded interface and pull-out. Thus, increases in the number, diameter and debonded length of such

bridging reinforcements should enhance the toughening effects [8–11].

In the self-reinforced silicon nitride ceramics, this involves the controlled incorporation of large ($>1\ \mu\text{m}$) diameter elongated grains [13, 14]. For instance, a bimodal (~ 0.5 and $\sim 2\ \mu\text{m}$) diameter distribution of the elongated grains yielded strengths $>1\ \text{GPa}$ and toughness values $>10\ \text{MPa m}^{1/2}$, while a uniform $\sim 0.5\ \mu\text{m}$ equiaxed grain size resulted in a strength of $\sim 600\ \text{MPa}$ and a toughness of $\sim 3.5\ \text{MPa m}^{1/2}$ [14]. Recent work has shown that a distinct bimodal diameter distribution of the elongated grains may not be required to achieve similar toughening effects [15]. In this work, a silicon nitride with a monomodal diameter distribution (average $\sim 1\ \mu\text{m}$) and one with a bimodal diameter distribution (~ 0.6 and $\sim 2\ \mu\text{m}$) exhibited toughness values of $\sim 10\ \text{MPa m}^{1/2}$, each with similar area fraction of reinforcing grains. The high toughness achieved with the smaller ($\sim 1\ \mu\text{m}$) reinforcing grains can probably be attributed to a greater degree of crystallographic texture of the reinforcing grains, since when the textures of the two microstructures are similar, the toughness is lower in the material with the smaller diameter reinforcing grains. This points out that orienting the reinforcing grains so they actively participate in the crack-bridging process can contribute to the level of toughness obtained. The effects of the diameter and texture of the reinforcing grains on the toughness are

* To whom all correspondence should be addressed.

E-mail address: Becherpf@ornl.gov (P.F. Becher)

‡ Now with United Technologies Research Center, East Hartford, CT, USA.

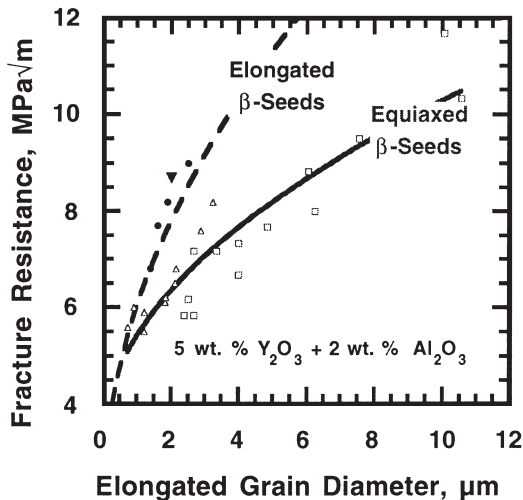


Fig. 1. The toughness of silicon nitride can be scaled with the diameter of the elongated reinforcing grains. The toughening effect in ceramics with randomly oriented reinforcements (equiaxed seeds, [3, 4]) can be increased by enhancing the alignment of these grains (elongated seeds, [6, 14]).

illustrated in Fig. 1. In summary, both toughening models and experiments reveal that tailoring the microstructure is a versatile method for developing substantially enhanced fracture properties, but only if attention is paid to the microstructural parameters affecting the bridging contributions.

Against this background, we must emphasize that, for these toughening mechanisms to be operative, it is imperative that the interface between the matrix and the reinforcing grains debond (or separate), Fig. 2. This debonding process must occur so that the crack tip is deflected along the grain face, rather than cutting through the elongated grain, while leaving intact elongated grains to bridge the crack in its wake. In the case of silicon nitride ceramics the microstructure consists of an amorphous silicate-based intergranular film (IGF) approximately 1 to 1.5 nm thick that surrounds all Si_3N_4 grains, including the elongated grains. The question then is how to tailor the structure or chemistry of the interfacial region to

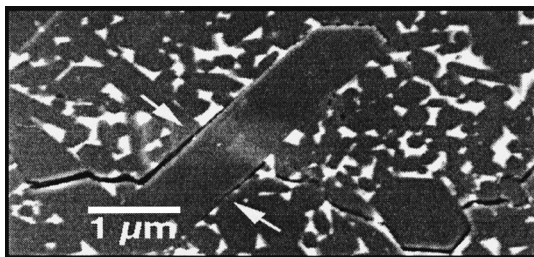


Fig. 2. The toughening effect observed in silicon nitride ceramics is associated with elongated grains that bridge the crack in the tip wake. Bridging by the grain occurs when the interface between it and the matrix separates or debonds (arrows). Each silicon nitride grain is surrounded by an amorphous intergranular film (white).

optimize the debonding process and, hence, the fracture toughness of these ceramics.

2. INTERFACIAL DEBONDING PROCESSES

Based on recent observations there appear to be at least two interfacial debonding processes in silicon nitride ceramics. In one, the introduction of appropriate anions generates crack-like defects within the amorphous intergranular film (IGF) (i.e., weakening the intergranular film by “crack formation in the IGF”) [16]. In the other process, the strength of the interface between the amorphous film and the elongated grains is found to depend on the growth of an epitaxial SiAlON layer at the interface—“interfacial strengthening” [17, 18]. The intent here is to focus discussion on the experimental and theoretical aspects of these two chemical/structural effects.

It is recognized that either of these debonding processes may be affected by the generation of thermal expansion mismatch stresses between the intergranular phase(s) and the silicon nitride. These stresses arise because the coefficients of thermal expansion of the amorphous IGF films are at least two times greater than those of the anisotropic beta grains. As a result, the interface along prismatic grain surfaces will be subjected to radial compression and the film will be subjected to tension. These radial compressive stresses could inhibit interfacial debonding along these critical interfaces. Earlier investigations showed that the radial compressive stresses are, at best, a secondary factor in the presence of SiAlON epitaxial layers [17]. When SiAlON is not present at the interface, the extent of debonding at the $\text{Si}_3\text{N}_4/\text{glass}$ interface is diminished by increases in the radial compressive stress [18]. In addition, the local tensile stresses, including those due to thermal expansion mismatch, are seen to promote the growth of crack-like defects introduced in the amorphous films containing fluorine [16]. The local residual stresses would then be a key component in the generation and growth of cracks within the intergranular film and debonding at the interface with the reinforcing phase.

Clearly, work to understand the effects of additives on crack formation in the IGF and interfacial strengthening (as well as on the high-temperature properties of the ceramic system, such as viscosity) has entered the regime of nanoscale chemistry, focusing predominantly on atomic-level phenomena that manifest themselves at the macroscopic scale in often dramatic ways. This evolution to the nanoscale in efforts to better understand IGF behavior is evidenced in the number of detailed characterization studies, such as those involving high-resolution transmission electron microscopy and electron energy-loss spectroscopy (e.g., [19]). Atomistic theoretical studies with first-principles [20, 21] and molecular dynamics [22, 23] modeling are, then, natural complements in the interpretation of experiments at this scale, and

much is being learned about atomic-level behavior both at the interface and within the IGFs.

2.1. Crack formation in the IGF

The process of IGF crack formation involves the formation of *weak bonds within the amorphous intergranular film*, for example by the addition of an anion such as fluorine, as discussed by Pezzotti *et al.* [16]. When the local density of these weakened bonds is sufficiently high, a crack-like feature forms, which grows in the presence of either an applied stress, a residual thermal expansion mismatch stress, or a combination of these stresses. According to the description of Pezzotti *et al.* [16], insertion of fluorine in the amorphous phase results in a pair of fluorine ions (difluorine), required to maintain the local charge balance, substituting in the position formerly taken by the oxygen linking the SiO_4 tetrahedra in the intergranular film (see Fig. 3). The fluorine pair is considered to move the tetrahedra apart due to the Coulomb repulsion between the two F^- ions, thus dilating the film, consistent with high-resolution electron microscopy (HREM) observations [19]. As a result of fluorine doping, oxygen-bridge linkages between tetrahedra are lost with each being replaced by a defect (i.e., missing bond) whose number density increases with fluorine content.

For the present study, the following first-principles atomic cluster calculations were made to provide an atomic-level description of the effects of substitution of difluorine for oxygen, from which two important features emerge: (1) strong Si–F bond formation (as expected on the basis of valency considerations) and (2) very weak interaction between the tetrahedra joined by the F–F pair. Here, the partial-wave self-consistent-field method [25] was used to solve the local density equations [26] precisely within an atomic cluster chosen to capture the essentials of the problem of interest: here, the energetics and structural effects of replacing a bridging oxygen atom linking two SiO_4 units by a pair of fluorine atoms. The chemical reaction steps involved in the interaction of CF_2 with the oxygen site in amorphous SiO_2 , with removal of the bridging oxygen atom and replacement with two fluorine atoms, is the subject of another study [27]. Here we compare the energy and structure for a “lattice fragment” of the SiO_2 glass



Fig. 3. Inserting a pair of fluorine ions in the position formerly taken by the oxygen linking the SiO_4 tetrahedra in the intergranular film results in the loss of the very strong oxygen link between tetrahedra. The very weak bond between the two fluorines is comparable to introducing a defect in the glass network.

made up of two oxygen-bridged SiO_4 tetrahedra with results for the difluorine-doped cluster.

Electronic structure and total energy calculations were carried out self-consistently, allowing charge density rearrangements, for the IGF reference SiO_2 cluster made up of two SiO_4 tetrahedra corner-linked through a bridging oxygen. Atoms were allowed to relax according to the calculated energy and force field, evaluated for each atom in the cluster. The fully relaxed fluorine-free cluster displays bond lengths in good (within 2%) agreement with experiment [28], justifying its use as a reference for determining dopant effects in the atomic cluster model. The total binding energy for this $\text{O}_3\text{Si}-\text{O}-\text{SiO}_3$ fragment (42.317 eV) reflects its high stability. Calculations of the energy of removal of the bridging oxygen atom show that its binding is strong (~ 6.40 eV) compared with the average binding energy of 6.05 eV per oxygen atom in the SiO_2 fragment. Similarly, for a *single* fluorine atom occupying the bridge site, the binding energy of fluorine is found to be ~ 1.40 eV less than that of oxygen. This tells us that the attack of silicon by fluorine alone in the glass would not disrupt the SiO_2 network.

Results for the cluster in which two fluorine ions are centered about the origin previously occupied by the bridging oxygen atom show the greatest stability with a binding energy of 47.432 eV. However, each of the very strong Si–F bonds is localized between fluorine and its nearest neighbor silicon, such that the two O_3SiF tetrahedra are only weakly interacting. Most of the binding energy originates within each O_3SiF unit. Most significant with regard to the IGF fracture behavior, these units become essentially non-interacting: only a very small force (≤ 0.85 eV/nm) is needed to separate these two tetrahedra beyond the local binding energy minimum of ~ 0.04 eV at an F–F distance of ~ 0.230 nm, Fig. 4. In contrast, the

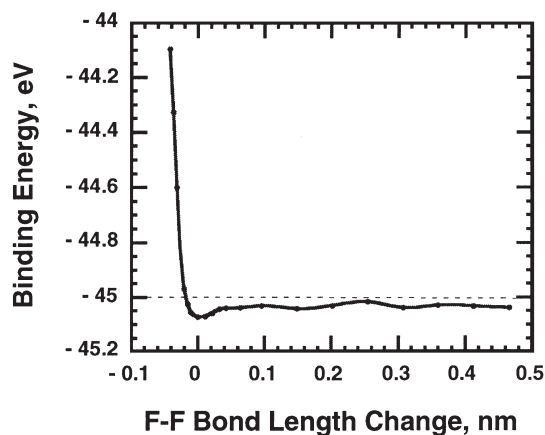


Fig. 4. The binding energy curve for the D_{3d} symmetry $\text{SiO}_3-\text{F}-\text{F}-\text{SiO}_3$ cluster as a function of separation of the tetrahedral units along the F–F axis. (The symmetry constraint raises the energy by ~ 2.3 eV relative to symmetry-relaxed values given in text). The zero of energy is for free atom constituents, and the separation is relative to equilibrium (F–F bond = 0.1193 nm).

tetrahedra of the oxygen-bridged reference cluster are bound so strongly to the joining oxygen atom that very large restoring forces (~ 41 eV/nm) act to return any displaced unit to equilibrium. In this analysis, IGF crack formation is a result of the fluorine pair substitution creating an extremely weak F–F bond and not a missing or dangling bond (plus a charge imbalance) that enhances crack growth in the amorphous phase. This enhanced crack formation and growth due to the fluorine reaction with the network is similar to that occurring when a water molecule interacts with the SiO₂ bonds at a crack tip in glasses [24].

In the difluorine structure, there is a strong repulsion when the F–F separation decreases below 0.185 nm and the fluorine densities overlap significantly (penetration beyond $\sim 30\%$ of the nominal ion radius). This repulsive force resists compression of the F–F bonds between the tetrahedra due to the van der Waals dispersion forces attempting to pull adjacent grains together [29]. The fact that the IGF is amorphous poses some problem for directly applying the calculated change in structure of the linked tetrahedra to the experimentally reported dilation of the IGF of 0.1 nm (e.g., see [19]). The increase in dimension is almost entirely in the F–F spacing, which becomes 0.243 nm. At first sight this seems too large, but if one incorporates the interactive forces between adjacent grains that define the IGF, film thicknesses are accurately given to within experimental precision (± 0.1 nm) for both the SiO₂ glass and the fluorine-doped film (e.g., [19]). Taken together, the studies of anion dopant effects in IGFs show that weakening of the amorphous network by anion additions results from interactions at the atomic level in the strictest sense: the interaction range involved in the replacement of oxygen by difluorine is distinctly localized to the region of the former oxygen-bridge bond. This suggests the possibility of debonding control with selectivity at the atomic level, since the effect of dopants is specific to a particular type of site in the IGF and the results of the doping are known.

2.2. Interfacial strengthening due to epitaxial SiAlON

The second process that controls debonding is associated with the strength of bonding across the glass/crystalline interface. In the experimental approach used here, an increase in the interface strength is reflected by a decrease in the critical angle between the plane of the propagating crack and the prism plane at which the crack starts to deflect up the interface [17, 18]. High-resolution, high-magnification scanning electron microscopy images of the whiskers embedded in the various glasses indicate that the debond crack does run along the crystalline/glass interface. Studies of both β -Si₃N₄ whiskers embedded in oxynitride glasses and self-reinforced silicon nitride ceramics reveal that the critical debond angle is modified by the formation of

an epitaxial β -Si_{6-z}Al_zO_zN_{8-z} layer between the β -Si₃N₄ grain and the amorphous IGF, Table 1.

Comparison of the critical debond angle with analysis of the radial compressive stresses imposed on the prismatic interfaces indicates that the radial stress is not a major factor when an epitaxial SiAlON layer is present, as mentioned earlier. This is clearly shown for the 55Si10Al35Y20N80O glass system by comparing the critical debond with and without an epitaxial SiAlON layer present, Table 1. In addition, reductions in the nitrogen content of the glasses, while having only a minor effect on the radial stress levels, exclude the formation of an epitaxial layer and interfacial debonding occurs quite readily then.

The observations summarized in Table 1 reveal that the introduction of aluminum and oxygen into this epitaxial layer increases the strength of the interface [17, 18]. At the same time, the fracture toughness of self-reinforced Si₃N₄ ceramics with identical microstructures is found to decrease with increases in aluminum and oxygen level in the epitaxial SiAlON layers [30]. As a result, the potential for differences in the types of bond that formed across the interface, seen schematically in Fig. 5, was examined as a source of the interface strength. In the presence of a SiAlON layer, both Si–O and Al–O bonds, as well as Si–N bonds, could form, and thus silicon, aluminum, oxygen and nitrogen atoms would participate in the bonding from both sides of the interface with the Si–Al–RE–O–N amorphous intergranular films. This would increase the density of bonding sites along the interface and suggests a mechanism for the rise in strength of the interface. While Al–N bonds are involved in the SiAlON crystal structure, there is little evidence for them in the oxynitride glasses [31, 32], and thus they were not included in the interface bonding considerations. On the other hand, the formation of Si–O, Al–O and Si–N bonds is well documented in the oxynitride glasses.

Earlier electronic structure calculations showed that the substitution of aluminum and oxygen into the lattice of β -Si₃N₄ reduces the total overlap population (a measure of electron bond density) to which the substituted atoms contribute, in keeping with a reduction of the mechanical properties of β -Si₃N₄ versus β -Si_{6-z}Al_zO_zN_{8-z} [33, 34]. However, more recent studies that include charge redistribution indicate that while the substitution of aluminum for a silicon in an Si₃N₄ unit results in a weaker Al–N bond, the strengths of other aluminum- and silicon-containing bonds in the structure actually increase [35]. In addition, crystal-orbital-based calculations have assessed the bonding of aluminum and oxygen to the β -Si₃N₄ surfaces and suggested stronger bonding of these elements to the prism faces, but only as compared with the basal surface [36].

The observed influence of the SiAlON composition on the interface strength motivated the current studies using first-principles atomic cluster calculations to address the following. (1) Why is the oxynitride

Table 1. Summary of the critical interfacial debond angles for the β -Si₃N₄/oxynitride glass

Sample	Critical debond angle (°)	Compressive stress on interface (MPa) ^a	Si _{6-z} Al _z O _z N _{8-z}	β -SiAlON predicted from phase equilibria
β-Si₃N₄ whiskers in oxynitride glass matrix				
<i>Composition (eq%)</i>				
55Si25Al20Y10N90O	~70	~350	0	No
55Si25Al20Y20N80O	~55	~320	1.0	Yes
55Si10Al35Y10N90O	~70	~515	0	No
55Si10Al35Y20N80O				
without SiAlON layer	~72	~530	0	Yes
with SiAlON layer ^b	~50	~530	0.15	
57Si43La20N80O	~68	~590	0	No
46Si27Al27La27N73O	~50	~555	1.6-2.0	Yes
41Si30Al29Yb23N77O	~55	~455	1.6-2.0	Yes
Self-reinforced β-Si₃N₄ with amorphous intergranular film				
<i>Additives (wt%) yttria/alumina</i>				
6.25/1.0	~75		0.01	Yes
5.0/2.0	~70		0.03	Yes
4.0/2.8	~60		0.06	Yes

^a Calculated stress based on measured values of thermal expansion coefficients, softening temperatures and Young's modulus of the glasses and silicon nitride (e.g., [18]).

^b Sample after additional nitrogen (5 MPa) anneal at 1680°C for 30 min to develop epitaxial layer.

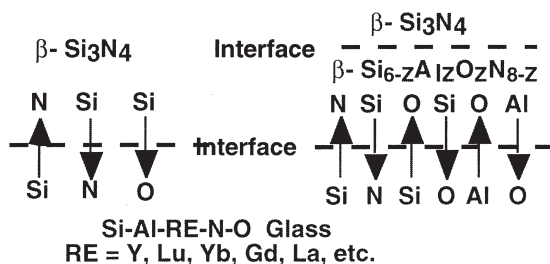


Fig. 5. As shown schematically here, only Si-N bonds are established in both directions across the interface in the case of the Si₃N₄/glass interface. When an epitaxial SiAlON layer forms, Si-O and Al-O bonds, as well as Si-N bonds, form in both directions across the glass/crystalline interface.

glass/ β -Si₃N₄ interface weak compared with the β -Si_{6-z}Al_zO_zN_{8-z}/glass interface? (2) What is the strengthening mechanism when Si_{6-z}Al_zO_zN_{8-z} forms at the interface? (3) What is the influence of composition on the interfacial strength in terms of atomic-level interactions?

The model structure used for this study was the basic tetrahedron, which is a common structural unit of both the crystalline phases (i.e., β -Si₃N₄ and β -Si_{6-z}Al_zO_zN_{8-z}) and the oxynitride glasses. The interfacial debonding of most interest here involves that parallel to the prism planes of the elongated reinforcing grains. A slice normal to these planes, shown schematically in Fig. 6, reveals that the atoms in the grain and the glass involved in bonding across the prism interfaces can also, indeed, be defined in tetrahedral units. Thus, one can use the simple tetrahedral unit building blocks to begin to describe the interfacial bonding and the effects of composition by altering the atomic species within the body-centered silicon- and aluminum-based tetrahedral clusters.

The partial-wave self-consistent cluster method [25] was used to solve local density equations for

such tetrahedral cluster models. This allows one to determine the energy and force field changes that would occur by a variety of atomic substitutions to gain a first approximation of the influence of composition on the interface cohesion. To achieve an atomic-level understanding of compositional effects, the electronic structures, total energies and atomic force fields were calculated to high accuracy using only the atomic numbers and parameters describing the local exchange correlation approximation (plus gradient corrections) as inputs.

Then the source was sought for the increase in interface strength with the formation of an epitaxial Si_{6-z}Al_zO_zN_{8-z} layer at the interface and the rapid rise in strength over a compositional range of $z = 0$ to ~ 0.2 (i.e., increasing substitution of aluminum for silicon and oxygen for nitrogen). The influence of aluminum and oxygen can be addressed by determining how the binding energy of the basic body-centered silicon (and aluminum) tetrahedra are affected by variations in the nitrogen-to-oxygen ratio. As seen in Fig. 7, the trend is for the binding energy to increase with substitution of oxygen for nitrogen in both the silicon- and aluminum-based tetrahedra. At the same N/O ratio, the silicon-based tetrahedra do exhibit higher binding energies than the aluminum-based tetrahedra. However, the AlO₃N and AlO₄ tetrahedra exhibit greater binding energies than do the SiN₄ and SiON₃ tetrahedra. In fact, the binding energy of the AlO₄ unit closely rivals that of the SiO₄ unit. On the other hand, the AlN₄ and SiN₄ tetrahedra are the most weakly bound units.

The above trends of increasing binding energies within both silicon- and aluminum-based tetrahedra with increasing substitution of oxygen for nitrogen are confirmed by additional calculations based on two and three corner-connected tetrahedra with oxygen substituted for nitrogen and aluminum for silicon.

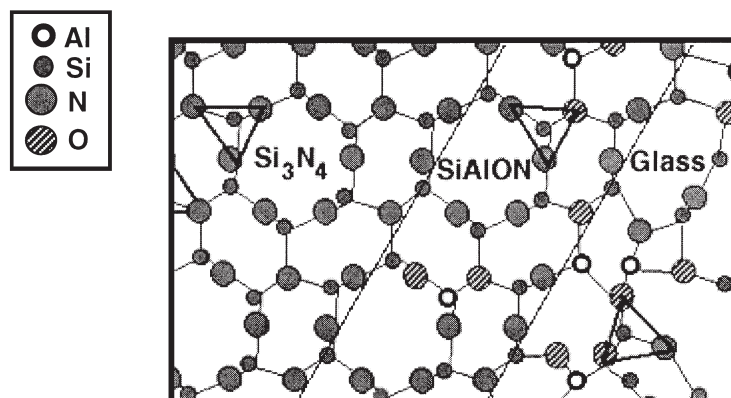


Fig. 6. The atomic structure involved in bonding across the prism planes is shown in the cross-section parallel to the basal plane of Si_3N_4 that cuts across the $\text{Si}_3\text{N}_4/\text{SiAlON}$ and $\text{SiAlON}/\text{glass}$ interfaces. Basic to all three components are the simple silicon-based and aluminum-based body-centered tetrahedral unit cells, which are used in the atomic cluster calculations to describe bonding at the interface.

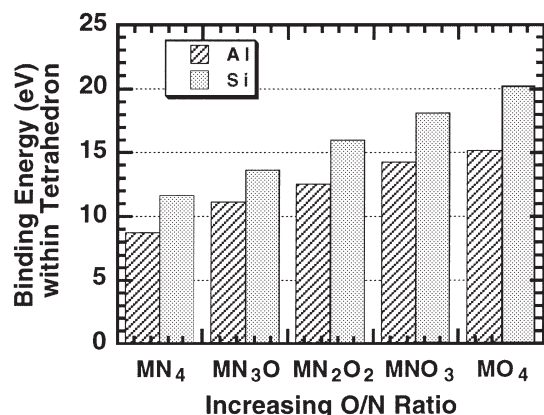


Fig. 7. First-principles calculations of the binding energy reveal a continuous increase with substitution of oxygen for nitrogen in both the silicon- and aluminum-based tetrahedra. While the silicon-based tetrahedra exhibit greater binding energies than do their aluminum-based counterparts, the oxygen-rich AlO_3N and AlO_4 tetrahedra exhibit greater binding energies than do the oxygen-deficient SiN_4 and SiON_3 tetrahedra.

These, then, further support the strengthening of the interface bonding by the addition of Si–O and Al–O bonding across the interface as first suggested in Fig. 5. At the $\beta\text{-Si}_3\text{N}_4/\text{glass}$ interfaces, silicon on the Si_3N_4 surface can bond to oxygen in the glass, while Si–N bonds can form in both directions across the interface. With an epitaxial $\text{Si}_{6-z}\text{Al}_z\text{O}_z\text{N}_{8-z}$ layer at the interface, Si–O bonds, the strongest bonds, can form across the interface in both directions. In addition, these are supplemented by Al–O bonds, the second strongest bonds in the series, which can be formed in either direction across the interface. Both the greater strengths of these oxide bonds and the fact that they can involve silicon and aluminum atoms present on both sides of the interface contribute to the increase in interfacial strength and resistance to debonding observed with the increasing substitution of aluminum and oxygen in the interfacial $\text{Si}_{6-z}\text{Al}_z\text{O}_z\text{N}_{8-z}$ layer.

3. SUMMARY

Interfacial debonding, which is a key step in crack-bridging mechanisms, appears to involve at least two processes. When fluorine is incorporated into the amorphous intergranular film, the glass network is weakened, which allows a propagating crack to bypass the reinforcing grains without cutting through them. In the presence of SiYAl oxynitride intergranular glass films, reductions in the Al/Y ratio decrease the aluminum and oxygen content of the epitaxial $\text{Si}_{6-z}\text{Al}_z\text{O}_z\text{N}_{8-z}$ layer on the Si_3N_4 grains and debonding is enhanced.

Atomic cluster calculations show that the substitution of two fluorine atoms in the place of the oxygen linking two SiO_4 tetrahedra results in (1) fluorines that are strongly bonded within each tetrahedra and (2) weak bonding between the two fluorine atoms, which are energetically favored to rest on the axis between the silicon atoms. As such, the calculated structure for the oxygen-linked and the fluorine-pair-linked tetrahedra yields intergranular film thicknesses in agreement with observations. The (at best) weak bond between the fluorine pair then acts like a defect in the glass network. The calculations show that the restoring force resisting the separation of the fluorine pair is extremely low. As a result, increases in the local density of such defects with fluorine additions will substantially weaken the intergranular glass network and, thus, allow cracks within the IGF to propagate around, rather than through, the reinforcing grains.

In the case of SiYAl oxynitride glass intergranular films, an increase in resistance to interfacial debonding occurs with the formation of the layer at the interface. Atomic cluster studies reveal that the binding energies of the SiN_4 tetrahedra increase as oxygen replaces the nitrogen, with SiO_4 exhibiting very high binding energies. The formation of $\text{Si}_{6-z}\text{Al}_z\text{O}_z\text{N}_{8-z}$ requires the incorporation of aluminum in place of silicon, and the binding energies of the aluminum-

based tetrahedra show the same increase with oxygen substitution for nitrogen. In fact, the AlO_4 tetrahedron has only slightly lower binding energy than does the SiO_4 tetrahedron. This increase in binding energies with oxygen substitution has an important impact on the interface strength.

When the glass is in contact with the Si_3N_4 grain, Si–N bonds can form in both directions across the interface; however, Si–O bonds will only occur between the silicon on the grain surface and oxygen in the glass. Thus opportunity to form the strongest bond (i.e., Si–O) is fairly limited. On the other hand, the growth of an $\text{Si}_{6-z}\text{Al}_z\text{O}_z\text{N}_{8-z}$ layer on the Si_3N_4 grains allows Si–O, as well as Si–N, bonds to form in both directions across the interface. The strong Si–O bonding will also be supplemented by the addition of nearly as strong Al–O bonding in both directions across the interface. Thus, the atomic cluster studies have established a relationship between composition and bond strength as a function of O/N ratio that provides insight into the role of composition on the debonding processes in the toughened silicon nitride ceramics.

Acknowledgements—This research was sponsored by the US Department of Energy, Division of Materials Sciences and Engineering, Office of Basic Energy Sciences, under contract DE-AC05-00OR22725 with UT-Battelle, LLC.

REFERENCES

- Himsolt, G., Knoch, H., Huebner, H. and Kleinlein, F. W. *J. Am. Ceram. Soc.*, 1979, **62**(1), 29.
- Lange, F. F. *J. Am. Ceram. Soc.*, 1979, **62**(7-8), 428.
- Kawashima, T., Okamoto, H., Yamamoto, H. and Kitamura, A. *J. Ceram. Soc. Jpn.*, 1991, **99**, 1.
- Mitomo, M. in *Proceedings: Science of Engineering Ceramics*, ed. S. Kimura and K. Niihara, Ceramic Society of Japan, Tokyo, 1991, p. 101.
- Hirao, K., Nagaoka, T., Brito, M. E. and Kanzaki, S. *J. Am. Ceram. Soc.*, 1994, **77**(7), 1857.
- Hirao, K., Nagaoka, T., Brito, M. E. and Kanzaki, S. *J. Ceram. Soc. Jpn.*, 1996, **104**, 55.
- Emoto, H. and Mitomo, M. *J. Eur. Ceram. Soc.*, 1997, **17**(4), 797.
- Becher, P. F., Hsueh, C. H., Angelini, P. and Tiegs, T. N. *J. Am. Ceram. Soc.*, 1988, **71**(12), 1050.
- Becher, P. F. *J. Am. Ceram. Soc.*, 1991, **74**(2), 255.
- Becher, P. F., Hsueh, C. H., Alexander, K. B. and Sun, E. Y. *J. Am. Ceram. Soc.*, 1996, **79**(2), 298.
- Sun, E. Y., Hsueh, C. H. and Becher, P. F. in *Fracture-Instability Dynamics, Scaling and Ductile/Brittle Behavior*, ed. R. B. Selinger, J. J. Mecholsky, A. E. Carlsson and E. R. Fuller, *MRS Proceedings*, Vol. 409 Materials Research Society, Boston, MA, 1996, p. 223.
- Evans, A. G. and McMeeking, R. M. *Acta metall.*, 1986, **34**(12), 2435.
- Li, C. W. and Yamanis, J. *Ceram. Eng. Sci. Proc.*, 1989, **10**(7-8), 632.
- Becher, P. F., Sun, E. Y., Plucknett, K. P., Alexander, K. B., Hsueh, C. -H., Lin, H. -T., Waters, S. B., Westmoreland, C. G., Kang, E. -S., Hirao, K. and Brito, M. *J. Am. Ceram. Soc.*, 1998, **81**(11), 2821.
- Hirao, K., Imamura, H., Watari, K., Brito, M. E., Toriyama, M. and Kanzaki, S. in *Science of Engineering Ceramics II*, ed. K. Niihara, T. Sekino, E. Yasuda and T. Sasa, Ceramic Society of Japan, Tokyo, 1999, p. 469.
- Pezzotti, G., Nishida, T., Kleebe, H. -J., Ota, K., Muraki, N. and Sergo, V. *J. Mater. Sci.*, 1999, **34**(7), 1667.
- Becher, P. F., Sun, E. Y., Hsueh, C. H., Alexander, K. B., Hwang, S. L., Waters, S. B. and Westmoreland, C. G. *Acta metall.*, 1996, **44**(10), 3881.
- Sun, E. Y., Becher, P. F., Hsueh, C. H., Painter, G. S., Waters, S. B., Hwang, S. L. and Hoffmann, M. *J. Act. mater.*, 1999, **47**(9), 2777.
- Kleebe, H. -J. *J. Ceram. Soc. Jpn.*, 1997, **105**(6), 453.
- Ching, W. -Y., Xu, Y. -N., Gale, J. D. and Rühle, M. *J. Am. Ceram. Soc.*, 1998, **81**(12), 3189.
- Kaneko, K., Yoshiya, M., Tanaka, I. and Tsurekawa, S. *Acta. mater.*, 1999, **47**(4), 1281.
- Blonski, S. and Garofalini, S. H. *J. Am. Ceram. Soc.*, 1997, **80**(8), 1997.
- Litton, D. A. and Garofalini, S. H. *J. Mater. Res.*, 1999, **14**(4), 1418.
- Michalske, T. A. and Freiman, S. W. *J. Am. Ceram. Soc.*, 1983, **66**(4), 284.
- Averill, F. W. and Painter, G. S. *Phys. Rev. B*, 1994, **50**(11), 7262.
- Jones, R. O. and Gunnarsson, O. *Rev. Mod. Phys.*, 1989, **61**(3), 689.
- Painter, G. S., unpublished.
- Jin, J., Yokoi, T., Miyaji, F., Sakka, S., Fukunaga, T. and Misawa, M. *Phil. Mag. B*, 1994, **70**(2), 191.
- Clarke, D. R. *J. Am. Ceram. Soc.*, 1987, **70**(1), 15.
- Sun, E. Y., Becher, P. F., Hsueh, C. -H., Waters, S. B., Plucknett, K. P., Hirao, K. and Brito, M. *J. Am. Ceram. Soc.*, 1998, **81**(11), 2831.
- Rouxel, T., Besson, J. L., Rzepka, E. and Goursat, P. *J. Non-Cryst. Solids*, 1990, **122**, 298.
- McMillan, P. F., Sato, R. K. and Poe, B. T. *J. Non-Cryst. Solids*, 1998, **224**, 267.
- Tanaka, I., Niihara, K., Nasu, S. and Adachi, H. *J. Am. Ceram. Soc.*, 1993, **76**(11), 2833.
- Tanaka, I., Nasu, S., Adachi, H., Miyamoto, Y. and Niihara, K. *Acta metall. mater.*, 1992, **40**(9), 1995.
- Ching, W. -Y., Huang, M. -Z. and Mo, S. -D., *J. Am. Ceram. Soc.*, 2000, **83**(4), 780.
- Dudsek, P. and Benco, L. *J. Am. Ceram. Soc.*, 1998, **81**(5), 1248.